Supporting Information

Crumpled B, F co-doped graphene nanosheets for the fabrication of all-solid-state flexible supercapacitors

Murugesan Sandhiya[a,b], Uma Kumar Kailash Veerappan [a] and Marappan Sathish[a,b]*

[a]Electrochemical Power Sources (ECPS) Division, CSIR-Central Electrochemical Research Institute, Karaikudi - 630003, Tamilnadu, India.

[b]Academy of Scientific and Innovative Research (AcSIR), Ghaziabad-201002, India.

E-mail: marappan.sathish@gmail.com; msathish@cecri.res.in

Corresponding author:

marappan.sathish@gmail.com; msathish@cecri.res.in

Experimental section

Materials

Graphite flakes powder (≤20μm, 99%), ammonium vanadate (NH_4VO_3), sodium vanadate (Na_2VO_3) purchased from Sigma-Aldrich, India. Sodium Nitrate ($NaNO_3$, 99 wt%), hydrazine hydrate (H_6N_2O, 99 wt%) potassium permanganate ($KMnO_4$, 99.5 wt%), hydrogen peroxide (H_2O_2, 30 wt%), 1-methyl 2-pyrrolidone (NMP) ($CH_3NC_4H_6O$), and poly acryclic acid (PAA) obtained using E-Merck, India. Sulfuric acid (H_2SO_4, 98 wt %) is acquired via Ranbaxy laboratories, Ltd. Poly (vinylidene fluoride) (PVDF) $(-CH_2-CF_2-)_n$ and 3-fluorobenzeneboronicacid purchased from Alfa Aesar, India. All the chemicals and reagents are used as received without any further purification. Deionized (DI) water is obtained from MILLIPORE water system.

Preparation of Graphene oxide (GO)

GO has been synthesized by graphite flakes using modified Hammer's method. In typical synthesis, 1 g of graphite flakes and 1 g of Na_2NO_3 are mixed with 50 ml H_2SO_4 in 1000 ml round bottom flask and stirred for ½ h. Afterwards, 6 g of $KMnO_4$ is added pinch by pinch under constant stirring and the temperature is maintained below 5 °C using ice bath. 80 ml of DI water was slowly added with vigorous stirring. The solution is further diluted by the addition of 200 ml of water followed by 6 ml of H_2O_2. The resultant mixture was stirred for 1 h. Then the filtered solution is filtered and washed with hot DI water several time until the pH of the solution become ~ 6. The product was dried under vacuum at 90 °C. The powder is re-dispersed with the known amount of DI water to make a GO solution.

Synthesis of B/F co-doped graphene (BFGO) by Supercritical fluid process:

3-fluorobenzeneboronicacid and GO dispersion in water (25 mL) were combined with 1:2 weight proportions and poured into stainless steel reactors. These reactors were vertically placed at 400 °C into a pre-heated furnace for 1 h. After the reaction, the reactors were quenched suddenly into the ice cold water. The resultant material was filtered and subsequently washed with water followed by ethanol. Then, the precipitate after the filtration was dried for overnight at 90 °C in hot air oven. The same procedure was followed for the preparation of BFGO-(1:3) and BFGO-(1:1) by changing the composition of 3-fluorobenzeneboronicacid and GO.

Materials characterization

The phase formation for all the synthesized powder materials were confirmed using powder X-ray diffraction (XRD) measurements via a BRUKER D8 ADVANCE X-ray Diffractometer with Cu K_α radiation (α=1.5418 Å). The 2θ values for the measurement of XRD are 10-70° in steps of 0.02° with a count time of 0.2 s. X-ray photoelectron spectroscopic analysis is carried out using Thermo Scientific MULTILAB 2000 base system with X-ray, Auger and ISS attachments containing Twin Anode Mg/Al (300/400W) X-ray source. The chemical nature and degree of defects in BFGO are characterized using a laser Raman system (RENISHAW I via laser Raman microscope) equipped with a semiconducting laser with a wavelength of 633 nm. The surface morphology of the samples analyzed using field-emission scanning electron microscopy (FE-SEM) using Carl Zeiss AG (Supra 55VP) with an acceleration voltage of 5 – 30 kV. The particle size and dispersion of all the prepared materials are examined using transmission electron microscope (TEM, Tecnai^{TM} G^2 20) working at an accelerating voltage of 200 kV.

Electrochemical characterization

Electrochemical characterization for the prepared samples were carried-out using a three-electrode setup in 1 M H_2SO_4. Among them, the best sample is tested with NH_4VO_3 redox additive dissolved in 1 M H_2SO_4 electrolyte. A slice of Pt foil and Hg/Hg_2SO_4 are employed as counter and reference electrode, respectively. Graphite foil was used as current collector as well as substrate for working electrode. For working electrode preparation, 75 wt% of ABGO sample, 20 wt% of super P carbon and 5 wt% of polyvinylidine fluoride binder were mixed and dispersed in N-methyl pyrrolidone. Approximately, 3 mg of the electrode material was coated over the graphite foil and the resulting electrode is kept in oven for drying at 80 °C for 6 h. For full cell studies and flexible device (single cell), total active mass of the cell is ~4 mg. All electrochemical experiments were performed by BioLogic SP-300 Modular Research Grade Potentiostat/Galvanostat/FRA electrochemical work station.

Mathematical formula for specific capacitance calculation from CD curve:

The specific capacitance of all the electrode materials was calculated from the data obtained from CD plot using the following equation:

$$C_{sp} = \frac{I \times t}{m \times \Delta V} \quad (1)$$

Where *C*-indicates the specific capacitance of the electrode [F/g], *m*-represents the mass of active material [g], *I*-denotes the galvanostatic discharge current [A], ΔV-signifies the potential window [V] and *t*-symbolises the discharge time [s].

Mathematical formula for energy density and power density of fabricated device:

The mathematical expression for the energy density and power density for a given supercapacitor device is mentioned as shown below.[22]

$$E = \frac{C(\Delta V)^2}{2 \times 4 \times 3.6} \quad (2)$$

$$P = \frac{E_t}{\Delta t} \times 3600 \quad (3)$$

Where E, ΔV, C, P and Δt specifies the energy density, operating cell voltage, the total capacitance of the full cell, power density and discharge time (s), respectively.

Preparation of redox additive based polymer gel electrolyte

In a typical gel electrolyte preparation, 2 g of PAA was slowly added to 25 ml of distilled water under constant stirring at 60 °C until it dissolves completely. Then, 25 ml of 1 M H_2SO_4 containing 0.01 M $NaVO_3$ was added into the PAA solution and stirred for 6 h to get $NaVO_3$/PAA/H_2SO_4 gel electrolyte. Same procedure is followed for the preparation of PAA/H_2SO_4 gel without adding $NaVO_3$.

Contribution of pseudocapacitance using Trasatti plot:

The contribution of pseudocapacitance arises by the doping of B and F can be quantified using Trasatti plot. The Trasatti method was used to differentiate the capacitance contribution from electrical double layer and pseudo-capacitive reactions. Cyclic voltammograms of BFGO were first performed with the scan rate ranging from 10 to 50 mV/s (Figure S6A). Then, corresponding gravimetric capacitances were evaluated based on the following equation:

$$C = {}^{S}/_{2 \times \Delta V \times \vartheta}$$

Where, C is the gravimetric capacitance of the BFGO electrode, S is the area enclosed by the CV curve, ΔV is the operating potential window, ϑ is the scan rate of the CV curve (V s^{-1}).

The plot of reciprocal of gravimetric capacitance and square root of scan rate gives the linear relationship. Data points collected at larger scan rates deviated from this linear

relationship due to intrinsic resistance of the electrode and deviation from semi-infinite ion diffusion. These deviated data points were masked during linear fitting (Figure S6B).

The "total capacitance" equals the sum of electrical double layer capacitance and pseudocapacitance. Plotting the gravimetric capacitances (C) against the reciprocal of square root of scan rates should also give a linear correlation described by the following equation (if assuming a semi-infinite diffusion of ions):

$$C = \ constant \times v^{1/2} + \ C_{EDL}$$

where C, ϑ and C_{EDL} is the experimental gravimetric capacitance, the scan rate and the electrical double capacitance, respectively. Linear fit the plot and extrapolate the fitting line to y-axis gives the maximum electrical double layer (Figure S6C). Subtraction of C_{EDL} from C_T yields the maximum pseudocapacitance (Figure S6D).

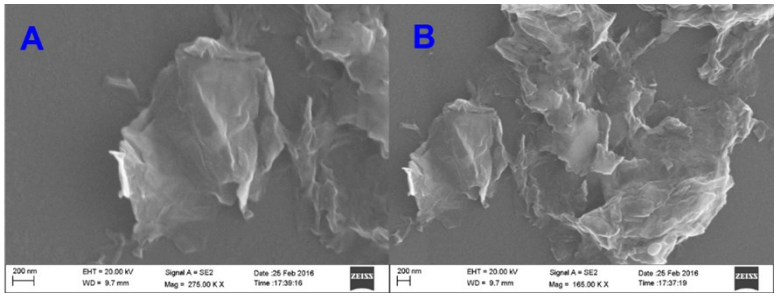

Figure S1. (A, B) FESEM images of RGO

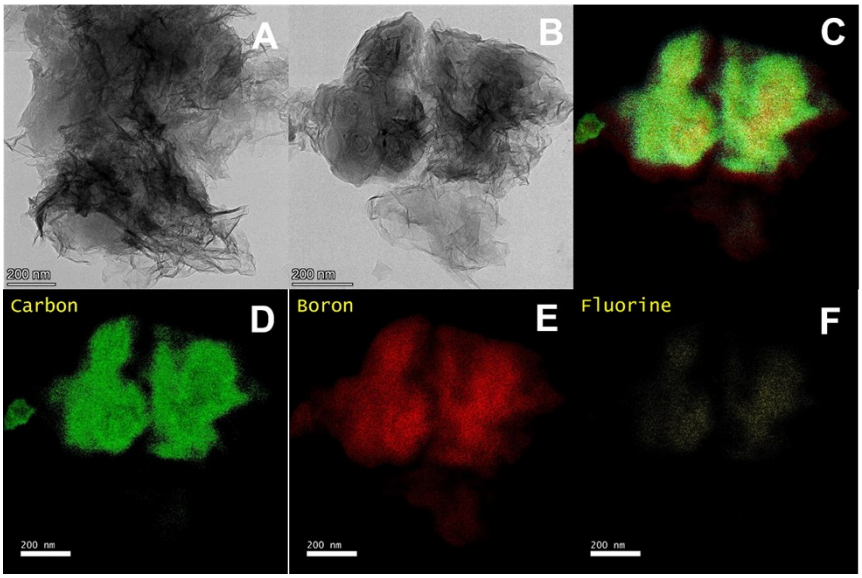

Figure S2. EFTEM (A-B) images, (C-F) Mapping of BFGO.

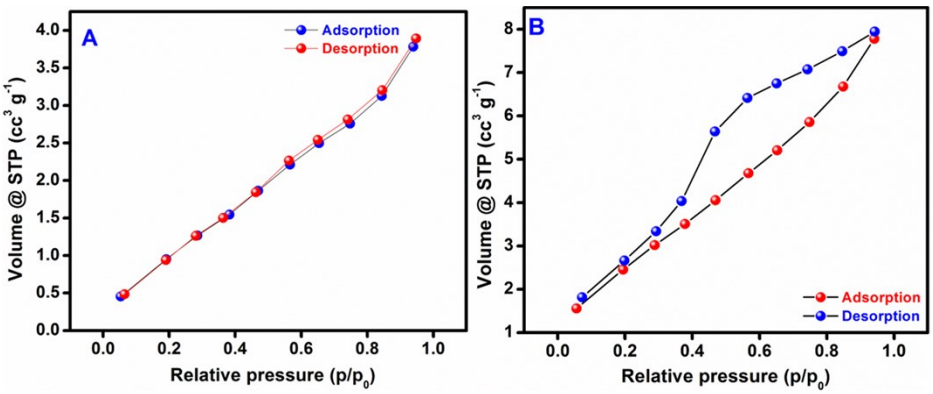

Figure S3. BET profile of (A) RGO and **(**B**)** BFGO.

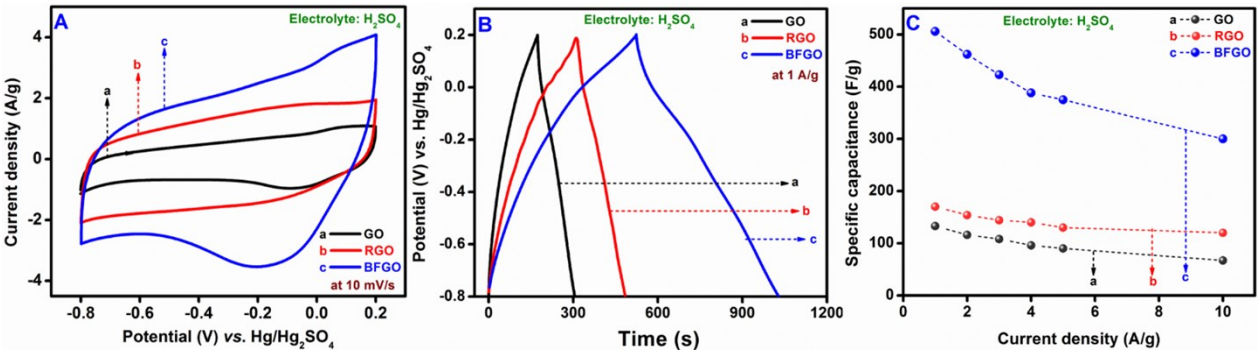

Figure S4. (A) CV (10 mV/s), (B) CD (1 A/g), and (C) Specific capacitance *vs.* current density profiles of (a) GO, (b) RGO, and (c) BFGO in H_2SO_4 electrolyte.

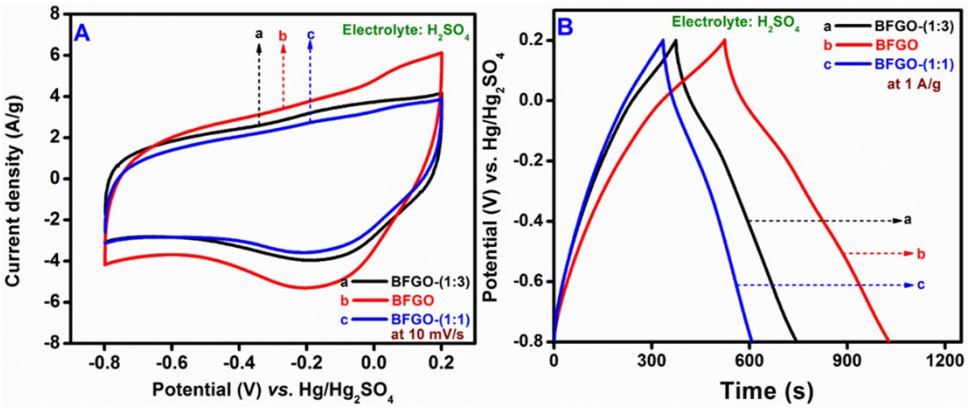

Figure S5. (A) CV (10 mV/s), and (B) CD profile (1 A/g) of (a) BFGO-(1:3), (b) BFGO, and (c) BFGO-(1:1).

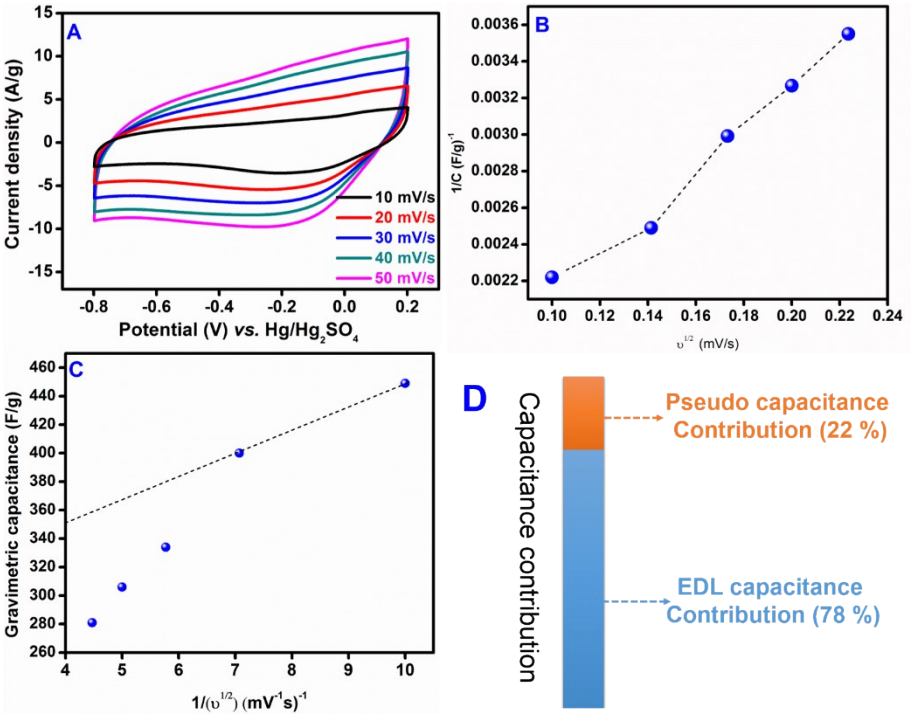

Figure S6. (A) CV profile of BFGO at various scan rates (B) Plots of reciprocal of gravimetric capacitance (C^{-1}) against square root of scan rate ($v^{1/2}$), (C) Plots of gravimetric capacitance (C) against reciprocal of square root of scan rate ($v^{-1/2}$), (D) Contribution of EDL and pseudocapacitance.

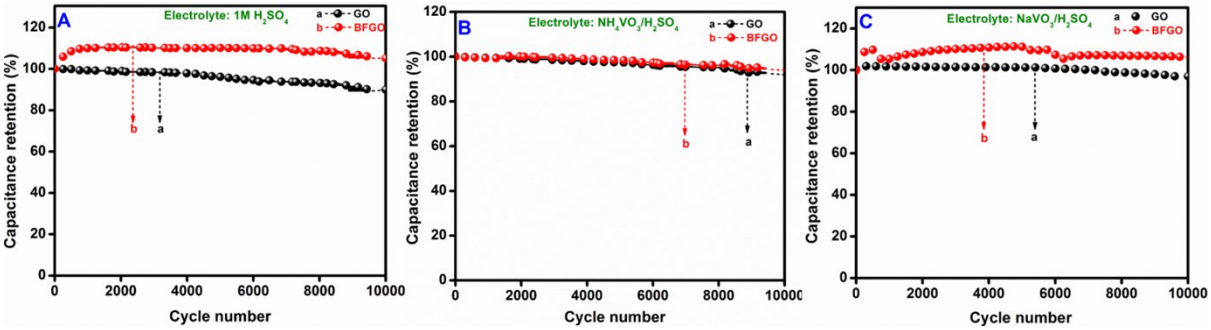

Figure S7. Long cycle stability of (a) GO and (b) BFGO in (A) H_2SO_4, (B) $NaVO_3/H_2SO_4$, and (C) NH_4VO_3/H_2SO_4.

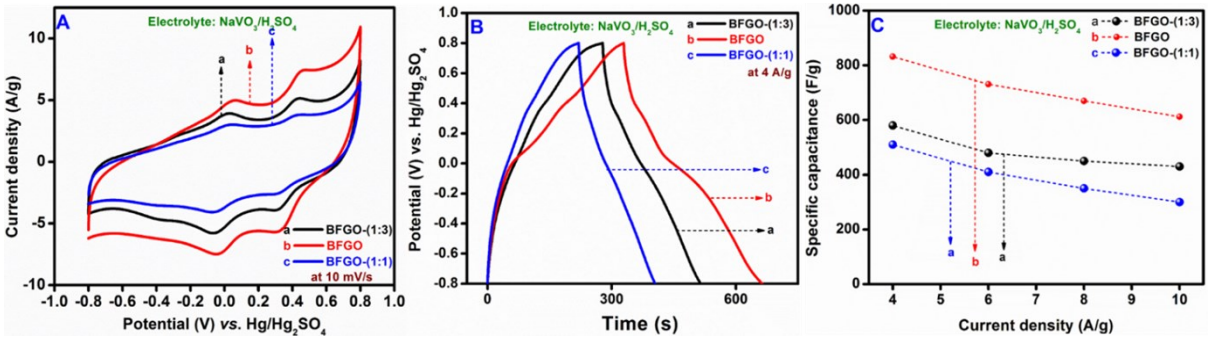

Figure S8. (A) CV, (B) CD, and (C) Plot of specific capacitance *vs.* current density.

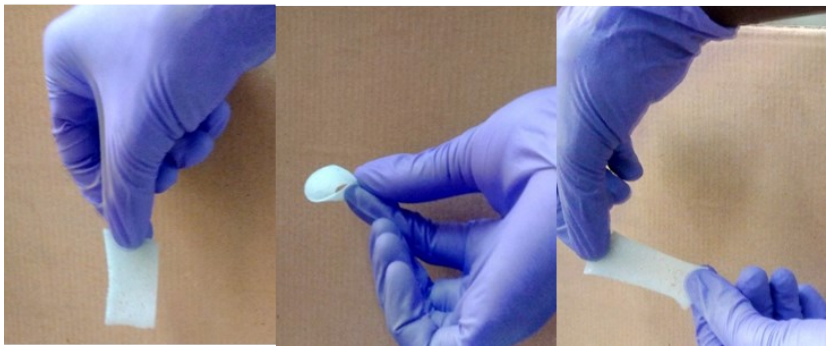

Figure S9. Photograph of foldable, bendable and stretchable nature of solid-state $NaVO_3/PAA/H_2SO_4$ electrolyte.

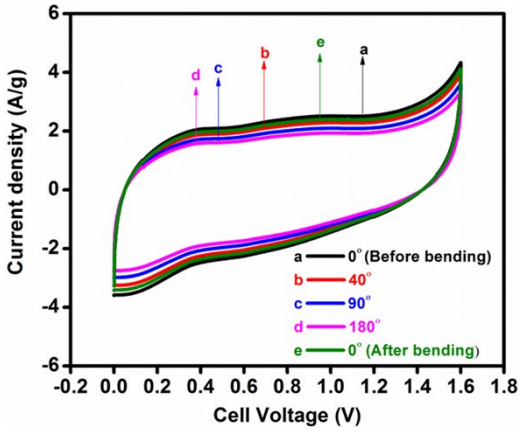

Figure S10. CV of ASFS device (at 10 mV/s) under different bending deformations.

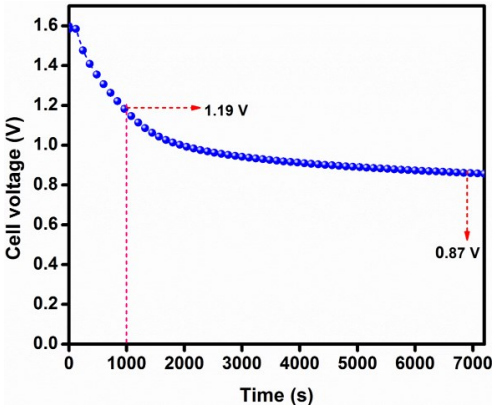

Figure S11. Self-discharge measurement of flexible solid-state device.

Table S1. The amount of B and F in BFGO with ratio of 1:2 of dopant source and GO.

Name of the element	At. %
C1s	79.53
O1s	17.17
B1s	1.95
F1s	1.35

Table S2. Specific capacitance of GO, RGO, and BFGO at different current densities using H_2SO_4 as an electrolyte.

Material	Specific capacitance (F/g) at different current densities (A/g) in H_2SO_4					
	1 A/g	2 A/g	3 A/g	4 A/g	5 A/g	10 A/g
GO	133	116	10	96	90	67

RGO	170	154	144	140	130	120
BFGO	506	462	423	388	375	300

Table S3. Capacitance retention of GO and BFGO in different electrolytes over 10,000 cycles.

Material	Capacitance retention in different electrolytes (%)		
	H_2SO_4	NH_4VO_3/H_2SO_4	$NaVO_3/H_2SO_4$
GO	90	92	97
BFGO	105	94	106

Table S4. Specific capacitance of GO, RGO, and BFGO in $NaVO_3/H_2SO_4$ at different current densities.

Material	Specific capacitance (F/g) at different current densities in $NaVO_3/H_2SO_4$			
	4	6	8	10
GO	252	228	220	187
RGO	455	412	340	290
BFGO	832	731	670	612

Table S5. The specific capacitance of different compositions of BFGO materials at various current densities.

Material	Specific capacitance (F/g) at different current densities in $NaVO_3/H_2SO_4$			
	4 A/g	6 A/g	8 A/g	10 A/g
BFGO-(1:3)	580	480	450	430
BFGO	832	731	670	612
BFGO-(1:1)	510	410	350	300

Table S6. Comparison of electrochemical performances of various co-doped graphene in different electrolytes.

Sl. No.	Material name	Synthesis method	Electrolyte	Specific capacitance (F/g)	Energy density (Wh/kg)	Capacitance retention	Ref.
1	NFG	ST	6 M KOH	345.4 at 1 A/g	7.99	87.7% Over 10,000 cycles	1
2	NPG	TA	6 M KOH	219 at 0.25 A/g	8.2	86% after 20,000 cycles	2
3	NPG	HT	6 M KOH	416 at	22.3	94.6% after 10,000 cycles	3
4	NPG	HT	1 M H_2SO_4	183 at 0.05 A/g	11.33	94% over 10,000 cycles	4
5	NSG	CO	1 M Na_2SO_4	442 at 0.5 A/g	~ 23.85	98.6% after 10,000 cycles	5
6	NSG	HT	1 M Na_2SO_4	536 F /g	14.8	94.25% after 7500 cycles	6
7	NSG	electron-beam (EB) based method	6 M KOH	60.1 at 1 A/g	8.3	83% after 25,000 cycles	7
8	NSG	plasma treatment	6 M KOH	307.4 at 1 A/g	9.33	83% after 10 000 cycles	8
9	NSG	TA	6 M KOH	305 at 1 A/g	28.44	95.4% after 10,000 cycles	9
10	**BFGO**	**SCF**	**1 M H_2SO_4**	**510 at 1 A/g**			**This work**
			$NaVO_3/H_2SO_4$	**832 at 4 A/g**			
			$NaVO_3$/PAA/H_2SO_4		**24**	**90% after 20000 cycles**	

Footnote: NFG-N, F co-doped graphene, NPG-N, P co-doped graphene, NSG-N, S co-doped graphene, ST-solvothermal, HT-hydrothermal, TA-thermal annealing and CO-chemical oxidation.

References

1. Y. Chen, Y. Li, F. Yao, C. Peng, C. Cao, Y. Feng, W. Feng, *Sustainable Energy Fuels*, 2019, 3, 2237-2245.
2. K. Xia, Z. Huang, L. Zheng, B. Han, Q. Gao, C. Zhou, H. Wang, J. Wu, *J. Power Sources*, 2017, 365, 380–388.
3. H. Cheng, F. Yi, A. Gao, H. Liang, S. Dong, Z. Xiaoping, H. Chun, Z. Zhenhua, *ACS Appl. Energy Mater.* 2019*, 2,* 4084−4091.
4. Y. Wen, T. E. Rufford, D. Hulicova-jurcakova, L. Wang, *ChemSusChem* 2016, 9,513–520.
5. G. Karthikeyan, B. Jayaraman, D. T. Tran, H. K. Nam, H. L. Joong, *Chem. Eng. J.* 2017, 312, 180-190.
6. Q. T. Ngoc, K. K. Bong, H. W. Moo, H. Y. Dae, *ChemSusChem* 2016*,* 9*,* 1–9.
7. C. Lingli, H. Yiyang, Q. Dandan, Z. Ying, W. Hao, J. Zheng, *Electrochim. Acta,* 2017, 259, 587-597.
8. M. Yuanling, M. Yulong, W. Qi, *ACS Sustainable Chem. Eng.* 2019, 7, 7597−7608.
9. A. Taslima, M. M. Islam, N. F. Shaikh, H. Enamul, I-M. Andrew, K-L. Hua, K. Konstantin, D. Shixue, ACS *Appl. Mater. Interfaces* 2016, 8, 2078-2087.